

Order parameter of a nematic liquid crystal on a rough surface

R. Barberi and G. Durand

Laboratoire de Physique des Solides, Université de Paris-Sud, Bâtiment 510, 91405 Orsay CEDEX, France

(Received 25 September 1989)

We measure the surface order parameter S_s at the interface between the nematic liquid crystal *p*-methoxy-benzylidene-*p*-*n*-butyl-aniline and a rough glass plate. Roughness is induced by oblique evaporation of SiO. We observe a critical decrease of S_s when the surface roughness increases, just above the transition from planar to oblique orientation. This experiment supports the ordoelectric model to explain the oblique orientation of the nematic liquid crystal.

Anisotropic interactions between nematic-liquid-crystal (NLC) molecules and a bounding wall can determine the direction of one or more spontaneous nematic orientations on the limiting surface. It has been known for a long time that rubbing, dielectric material oblique evaporation, and other methods which produce a grooved surface, can induce a uniform alignment of NLC.¹ The physical processes governing these orientations are not really understood and remain a challenge in liquid-crystal surface physics. In particular, obliquely evaporated SiO layers can align the NLC director \mathbf{n} ($n^2=1$) parallel to, or at an oblique angle from, a glass substrate.² The parallel (planar) alignment was first explained by Berreman³ and de Gennes⁴ using an elastic model. Molecules were assumed to align parallel to the local surface. This gives rise to an excess of elastic energy of NLC aligned perpendicular to "grooves" compared with the parallel alignment. In this elastic model the order-parameter modulus S of the NLC was assumed uniform and only \mathbf{n} was considered to vary in space, from the boundary geometrical constraint. Later on, the same model has been extended⁵ to explain the oblique (tilted) surface orientation of NLC. The director was supposed to align, near the wall, parallel to oblique "needles," which seems indeed to have been observed by electron microscopy.⁶ Obviously, for this model to work, needles dimensions or grooves spacing should be macroscopic, which is not really the case, since surface irregularities may have dimensions down to 100 Å.⁷

Recently, it has been discovered⁸ that the NLC orientation on obliquely SiO evaporated glass plates exhibits a continuous transition from a planar to an oblique orientation when SiO thickness increases. In a transition region, two easy oblique directions are observed. They are symmetrical compared to the normal plane of evaporation and finally merge into the classical oblique orientation. This transition and the subsequent saturation of obliquity for thick evaporation were explained by an order electric model.⁸ In this model the surface roughness is assumed to decrease the NLC surface order parameter S_s . S will vary close to the surface over a thickness ξ , the coherence length of the nematic-isotropic transition⁴ (ξ is a few 100 Å). The resulting gradient of order builds a surface order electric polarization,⁹ which induces a

director tilt, to minimize its electrostatic self-energy. The thickness integral of these energies over ξ is considered in this model as a contribution to the surface anchoring energy of the nematic liquid crystal.

To explain that S_s could be weak close to a rough surface, the Berreman-de Gennes model has been extended¹⁰ to the case $q\xi > 1$, where the wavelength $2\pi/q$ of surface undulations becomes shorter than ξ . For $q\xi > 1$, melting costs less free energy than curvature, i.e., $S_s < S$ in the bulk.

There are now two completely different models to describe the orientation induced by rough surfaces. The knowledge of S_s could help to choose between them. In the literature there is some qualitative indication about the possible existence of partial melting close a rough surface.¹¹⁻¹⁴ But measured quantities are integrated and the estimation of S_s is indirect. It is also possible to find some measurement of S_s , but they are performed at temperature very close to the clearing temperature T_c ,¹⁵⁻¹⁷ with only one exception,¹⁸ criticized in Ref. 16. In this article we present a direct measurement of S_s versus the surface roughness on SiO oblique evaporated glass plates, in the case of oblique NLC orientation, at room temperature. S_s is obtained from the measurement of the surface twist produced by an external uniform electric field, from its linear flexoelectric coupling with the NLC.

The flexoelectric behavior of NLC is essentially of quadrupolar origin.¹⁹ We can write the flexoelectric polarization \mathbf{P}_f as $\mathbf{P}_f = -\nabla \cdot \underline{\mathbf{Q}}$, with $\underline{\mathbf{Q}} = \frac{3}{2}(-e_0)S(\mathbf{nn} - \underline{\mathbf{I}}/3)$, where $-e_0$ is the quadrupolar density of a completely aligned nematic phase, S is the orientational order parameter, and $\underline{\mathbf{I}}$ is the unit matrix. When a uniform electric field \mathbf{E} is applied, we can write the flexoelectric contribution \mathcal{F}_f to the volume free energy as

$$\begin{aligned} \mathcal{F}_f &= \int_V -\mathbf{E} \cdot \mathbf{P}_f dv = \int_V \mathbf{E} \cdot (\nabla \cdot \underline{\mathbf{Q}}) dv \\ &= \int_V \nabla \cdot (\mathbf{E} \cdot \underline{\mathbf{Q}}) dv \\ &= \int_{\sigma_v} \mathbf{E} \cdot \underline{\mathbf{Q}} \cdot \mathbf{N} d\sigma, \end{aligned}$$

where V is the integration volume, σ_v is the surface around V , and \mathbf{N} is the normal external to σ_v . Using the geometry of Fig. 1, we write

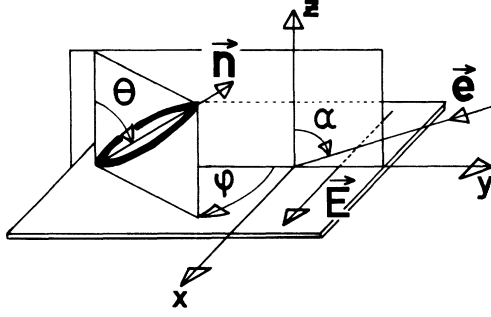


FIG. 1. Lower plate (\hat{x}, \hat{y}) geometry. \mathbf{e} is the evaporation direction.

$$\begin{aligned} \mathcal{F}_f &= \int_{\sigma_v} \frac{3}{2} (-e_0) S (\mathbf{E} \cdot \mathbf{n}) (\mathbf{n} \cdot \mathbf{N}) d\sigma \\ &= \int_{\sigma_v} -\frac{3}{2} (-e_0) S E (\sin\theta) (\cos\theta) (\sin\varphi) d\sigma, \end{aligned}$$

where θ and φ are the polar and azimuthal angles of the director. The flexoelectric effect gives only a surface term, linear versus the imposed electric field. In the transition region, the surface elastic energy presents two minima, at $\theta = \theta_s$ and $\varphi = \pm\varphi_s$. Under the flexoelectric effect, which depends also on θ and φ , the surface director will change in a complicated way, difficult to analyze. We restrict our analysis to the case of nondegenerate oblique anchoring $\theta_s, \varphi_s = 0$. By symmetry, φ and θ distortion are eigenmodes of the system and can be measured separately. We have chosen to observe the surface twist $\varphi_s(E)$. Our analysis will be reduced to the flexoelectric azimuthal torque per cm^2 $\Gamma_{f,z}$ which, on the lower plate, is written for small φ as

$$\Gamma_{f,z} = \frac{3}{2} (-e_0) S_s E (\sin\theta_s) (\cos\theta_s).$$

The other azimuthal torques which must be considered are the elastic torque $\Gamma_{e,z}$, from the anchoring energy minimum, and the dielectric torque $\Gamma_{d,z}$, from the anisotropy of dielectric constants $\epsilon_a = \epsilon_{\parallel} - \epsilon_{\perp}$. We model the anchoring energy in a phenomenological way and write, for small φ , the surface elastic torque as $\Gamma_{e,z} = [K/L(\theta)]\varphi_s$, where K is a normalization term equal to the bulk curvature elastic constant and $L(\theta)$ is the anchoring extrapolation length.⁴

In the presence of an external electric field and for small φ , the dielectric anisotropy gives for any volume element in the NLC the bulk azimuthal torque $\Gamma_D = (\epsilon_a/4\pi)E^2(\sin^2\theta)\varphi$. We assume that the electric coherence length $\xi_E = (1/E)(4\pi K/|\epsilon_a|)^{1/2}$ is smaller than the sample thickness d , but much larger than ξ . The dielectric volume torque can then be integrated through the volume, using for K and ϵ_a the bulk values, independent of the decrease of S at the surface. This gives a surface term $\Gamma_{d,z} = -(K/\xi)(\sin^2\theta_s)\varphi_s$ for the azimuthal variation. $\Gamma_{d,z}$ tends to align NLC molecules in the y - z plane if the dielectric anisotropy ϵ_a is negative and in the

x - z plane if ϵ_a is positive. In our case $\epsilon_a < 0$, so $\Gamma_{d,z}$ and $\Gamma_{e,z}$ are opposite to $\Gamma_{f,z}$. The balance of surface torques gives (in the small φ limit)

$$K \left[\frac{1}{L} + \frac{\sin^2\theta_s}{\xi_E} \right] \varphi_s = \frac{3}{2} (-e_0) S_s E (\sin\theta_s) (\cos\theta_s). \quad (1)$$

For small field $\xi_E > L$, we expect a surface twist

$$\varphi'_s = \frac{3(-e_0)LS_s \sin(2\theta_s)}{4K} E,$$

proportional to E , which allows us to measure LS_s . For large field $\xi_E < L$, we expect a saturation of the twist

$$\varphi''_s = \frac{3(-e_0)S_s}{\tan\theta_s} \left[\frac{\pi}{K|\epsilon_a|} \right]^{1/2}$$

because of the balance between Γ_f and Γ_d , independent from the surface anchoring strength. From φ''_s we can determine S_s . From Eq. (1), we obviously see that this flexoelectric method works only for $\theta \neq 0$ and $\theta \neq \pi/2$.

Is S_s the real surface order parameter? In the ‘‘ordoelectric’’ model of Ref. 8, one has introduced, to describe the tilt, the self-energy of a surface depolarizing field \mathbf{E}_s associated with the ordoelectric polarization. One could think that the uniform \mathbf{E} hypothesis is no longer verified close to the boundaries ($0 < z < \xi$), because of this surface field \mathbf{E}_s . In fact, \mathbf{E}_s is along \hat{z} and does not contribute to \mathbf{E} , which is parallel to \hat{x} . In our geometry, we can forget about \mathbf{E}_s and consider that the flexoelectric and elastic surface energies are real surface terms, as S_s itself.

Our experiment is performed with sandwich glass cells of about $30 \mu\text{m}$ thickness. Two parallel Mylar stripes serve as spacers. The SiO thickness δ , measured as in Ref. 20, varied between 90 and 520 \AA , for an angle of evaporation $\alpha = 75^\circ$, just above the transition region from planar to oblique orientation. The δ variation allows us in principle to change continuously the surface roughness from the relatively smooth untreated glass plate toward some saturation value.²¹ We use the *p*-methoxybenzylidene-*p*-*n*-butyl-aniline (MBBA), which is nematic at 20°C . As shown in Fig. 1, on the lower glass plate, two gold electrodes, parallel and at a distance of $40 \mu\text{m}$, are used to create the horizontal electric field \mathbf{E} , normal to the plane of evaporation. The upper plate is SiO evaporated with the same α and δ as the one of the lower plate. The cell is built with two glass plates antisymmetrically oriented with respect to the direction of evaporation. This results in homogeneous oblique orientation of the NLC director in the plane of evaporation.

TABLE I. Results from measuring θ , for $E = 0$, from various samples, from the apparent birefringence observed through a polarizing microscope.

δ (\AA)	90	100	130	260	520
θ (deg)	74.5	73.5	71.5	68.8	66.4

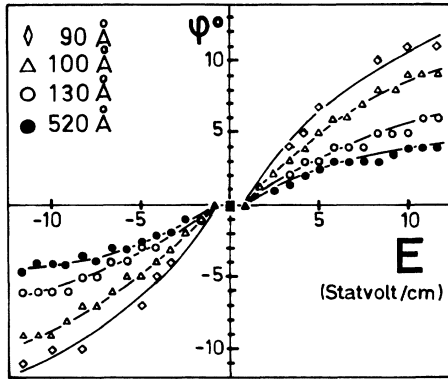


FIG. 2. Surface twist φ_s vs the applied electric field E . Solid lines are fitting hyperbolas.

We first measure θ , for $E=0$, from various samples, from the apparent birefringence observed through a polarizing microscope. The results are plotted in Table I and are obtained by using in our calculation the indices of refraction of MBBA from Ref. 22. Our measured value of the birefringence of a planar sample of MBBA is $\Delta n=0.23$. We now apply the field. θ changes a little and not uniformly. This is not important because θ and φ variations are orthogonal. We observe the surface twist at the center of the region where the electric field is applied, to better match the uniform electric field condition. We observe the input and output azimuthal angles φ , compared to the plane of evaporation, corresponding to the surface twist on the lower and upper plate, respectively, by determining the input and output optical eigenaxis of the sample, i.e., the absolute orientation of polarizer and analyzer twisted for maximum extinction of transmitted light ($\lambda=5460 \text{ \AA}$). We observe two opposite polar twists on both upper and lower surfaces. In the following we consider only the effect on the lower plate φ_s . We measure the twist angle φ_s versus the applied electric field, for different SiO evaporated thickness (Fig. 2). First note that between -1 and 1 statvolt/cm, there is no change in φ_s . The applied electric field is probably screened by ions. For stronger applied electric field, electrochemical effects break this screening and the surface twist appears. To analyze our data, we have suppressed the screened region and we have fitted the experimental points to calculate L and S_s , taking into account the effective applied electric field $|E'|=|E|-1$. The e_0 value is known from Ref. 19. As expected, φ_s is odd in E' . It shows a first linear change at small $|E'|$ and tends as expected towards an asymptotic value when $|E'|$ increases.

$L(\theta)$ does not change significantly versus δ (Fig. 3). Its small increase close to the transition region, although expected at the border of the φ degenerate region, is not reliable, with our present accuracy. L is found to be $2.0 \pm 0.3 \mu\text{m}$. Using $K=4 \times 10^{-7} \text{ dyn}$, the corresponding azimuthal anchoring energy W is about $2 \times 10^{-3} \text{ erg/cm}^2$. It is a factor of 2 smaller than the known zenithal anchoring energy²³ and corresponds to a “weak” anchoring strength.

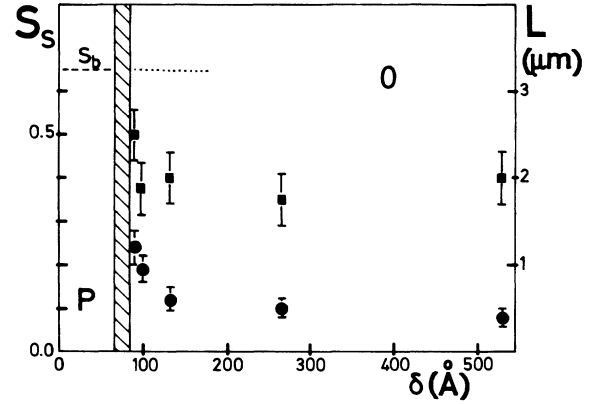


FIG. 3. Surface order parameter S_s (circles) and anchoring extrapolation length L (squares) vs the evaporated SiO thickness. The hatched area is the transition region where a twofold degenerate oblique orientation allows a continuous transition between the planar (P side) and the ordinary oblique (O side) orientations.

We show in Fig. 3 the measured surface order parameter S_s versus the evaporated SiO thickness δ just above the transition region with the twofold degenerate oblique orientation⁸ ($\delta=60-80 \text{ \AA}$). S_s decreases when δ , and hence the surface roughness, increases. For the planar anchoring (where we cannot use our method to measure S_s) at very small SiO thickness, S_s should be directly comparable with the bulk order parameter $S_b=0.65$.^{13,17} We deduce that the orientational transition region is characterized by an abrupt change of S_s from $S_b=0.65$ to 0.24 . There must then exist a large induced order-parameter gradient near the solid surface.

In conclusion, we have measured the surface order parameter S_s and the azimuthal surface energy versus the surface roughness in the case of tilted NLC anchoring, using the flexoelectric coupling of an applied dc electric field with the NLC. Our measurements are performed in the nematic phase of MBBA, at room temperature. We have observed an abrupt decrease of S_s versus the evaporated thickness δ of SiO evaporated glass surfaces. As the surface roughness must increase with δ from the relatively smooth untreated plate up to a saturation value, S_s is found to be a decreasing function of the roughness. Our observations, because of the expected order-parameter gradient near the surface, suggest that order electricity must be taken into account to explain the NLC oblique anchoring close to a rough solid surface.

We benefited from discussions with G. Barbero and technical support for SiO evaporation from M. Boix. One of us (R.B.) was partially supported by Consiglio Nazionale delle Ricerche (Italy) and NATO. R.B. is a member of GNSM-CISM-INFM, Unità di Cosenza (Italy). Laboratoire de Physique des Solides is “laboratoire associé au Centre National de la Recherche Scientifique (France).”

- *Permanent address: Università degli studi di Reggio Calabria, Facoltà di Ingegneria-via E. Cuzzocrea, 48-89128 Reggio Calabria, Italy.
- ¹A review on this subject is J. Cognard, *Mol. Cryst. Liq. Cryst. Suppl. Ser.* **1**, 1 (1982).
- ²E. Guyon, P. Pieranski, and M. Boix, *Lett. Appl. Eng. Sci.* **1**, 19 (1973).
- ³D. W. Berreman, *Phys. Rev. Lett.* **28**, 1683 (1972).
- ⁴P. G. de Gennes, *The Physics of Liquid Crystals* (Clarendon, Oxford, 1974).
- ⁵W. Urbach, M. Boix, and E. Guyon, *Appl. Phys. Lett.* **25**, 479 (1974).
- ⁶J. Cheng, G. D. Boyd, and F. G. Storz, *Appl. Phys. Lett.* **37**, 716 (1980).
- ⁷L. A. Goodman, J. T. McGinn, C. H. Anderson, and F. Di-geronimo, *IEEE Trans. Electron Devices* **24**, 795 (1977).
- ⁸M. Monkade, M. Boix, and G. Durand, *Europhys. Lett.* **5**, 697 (1988).
- ⁹G. Barbero, I. Dozov, J. F. Palierne, and G. Durand, *Phys. Rev. Lett.* **56**, 2056 (1986).
- ¹⁰G. Barbero and G. Durand (unpublished).
- ¹¹S. T. Wu and U. Efron, *Appl. Phys. Lett.* **48**, 624 (1986).
- ¹²H. Yokoyama, S. Kobayashy, and H. Kamei, *Mol. Cryst. Liq. Cryst.* **99**, 39 (1983).
- ¹³S. Faetti, M. Gatti, V. Palleschi, and T. J. Sluckin, *Phys. Rev. Lett.* **55**, 1681 (1985).
- ¹⁴G. Haas, M. Fritsh, H. Wohler, D. A. Mlynski, *Liq. Cryst.* **5**, 673 (1989).
- ¹⁵K. Miyano, *Phys. Rev. Lett.* **43**, 51 (1979).
- ¹⁶H. A. van Sprang, *J. Phys. (Paris)* **44**, 421 (1983).
- ¹⁷H. Yokoyama and H. A. van Sprang, *J. Appl. Phys.* **57**, 4520 (1985).
- ¹⁸H. Mada and S. Kobayashy, *Mol. Cryst. Liq. Cryst.* **66**, 57 (1981).
- ¹⁹J. P. Marcerou and J. Prost, *Mol. Cryst. Liq. Cryst.* **58**, 259 (1980).
- ²⁰J. L. Janning, *Appl. Phys. Lett.* **21**, 173 (1972).
- ²¹P. Meakin and R. Jullien, *Europhys. Lett.* **9**, 71 (1989).
- ²²E. B. Priestley, P. J. Wojtowicz, and P. Sheng, *Introduction to Liquid Crystals* (Plenum, New York, 1976).
- ²³L. Komitov and A. G. Petrov, *Phys. Status Solidi A* **76**, 137 (1983).